THE DECADAL CLIMATE VARIABILITY AND THE ANOMALOUS ENSO DEVELOPMENTS IN 1990S*

*ZHANG Qin*** (张 勤), *DING Yihui* (丁一汇) and *YI Lan* (伊 兰)

National Climate Center, Beijing 100081

Received July 5, 2001; revised October 23, 2001

ABSTRACT

By using the wavelet transform method, the ENSO (2—7 a) signal and the decadal variability (8—20 a) are filtered out from the long-term SST data sets in order to investigate characteristics of the decadal variability and its impact on the ENSO. It is found that there are two different kinds of decadal SSTA modes — horseshoe and horse saddle patterns in the tropical Pacific. The horseshoe pattern represents that the decadal SSTA variability in the central Pacific is in phase with that in the eastern Pacific. The horse saddle pattern is named that they are out of phase. The former constituted the decadal variability before 1990s and the latter mainly prevailed during 1990s. As the response of atmosphere to the ocean, two decadal wind patterns appear in association with the SST decadal modes. One is characterized by anomalous development of the zonal wind, the other by anomalous development of the meridional wind. These two kinds of modes can also be regarded as different phases of the decadal oscillation. Further studies have shown that the influences of the two kinds of modes on the ENSO are different. The horse saddle mode has a stronger impact on the ENSO than the horseshoe mode.

A possible mechanism for the influence of the decadal variability on the ENSO signal is presented. The central part of the thermocline along the equatorial Pacific moves up or down simultaneously with its eastern part while the decadal variability bears the horseshoe pattern. But the two segments of the thermocline in the central and eastern Pacific act oppositely while the decadal variability shows the horse saddle pattern. In this case it has an influence on the individual ENSO events by the superposition of the decadal variability.

Key words: decadal oscillation, ENSO, tropical Pacific

I. INTRODUCTION

In the 1980s, strong interannual variabilities were identified in the tropical Pacific from the regularly recurrent ENSO cycles, i. e., two El Nino events in 1982/1983 and 1986/1987, and two La Nina events in 1984/1985 and 1988/1989. Beginning from 1990, warm sea surface temperature anomaly (SSTA) persisted in the central equatorial Pacific near the dateline until 1995. During this period, three El Nino events took place with short time intervals. Maximum warming occurred in the spring of 1992, the spring of 1993, and around the end of 1994 (NCEP Climate Diagnostics Bulletin). The prolonged

* This work was supported by "National Key Program for Developing Basic Sciences" G1998040900 and the National Natural Science Foundation of China under Grant 49805007.

** Current address: Dr. Zhang Qin, Department of Meteorology, University of Hawaii, 2525 Correa Road, Honolulu, Hawaii 96822. qinz@soest.hawaii.edu.

warming from 1990 to 1995 was unprecedented (Trenberth and Hoar 1996). The 1997/1998 El Nino took place with major warming occupying the equatorial eastern Pacific. When the Nino3 index returned to normal in June 1998, the positive SSTA still existed in Nino1 and Nino2 areas for a long time.

During and after the TOGA, some dynamic numerical models were developed and utilized to predict tropical Pacific SSTA a year or more in advance, among which are the models of Cane et al. (1986), Barnett et al. (1988), Latif and Barnett (1996), Ji et al. (1994), and Balmaseda et al. (1994). Barnston et al. (1994) compared the skill of five models to forecast the Nino3 index with 6-month lead, and found that the averaged correlation coefficient between the predicted Nino3 index and the observed Nino3 index was 0.6 for the period of 1982—1993. Since 1991, most of the models seemed to be able to predict, in some extent, the warm events in 1991/1992 and 1997/1998 (Mason et al. 1999). However, none of the models was capable of capturing the 1993 and 1994/1995 warm events. It is no doubt that the forecast skill of the models, either dynamical or statistical, dropped appreciably in the 1990s compared to that in the 1980s (Ji et al. 1996; Balmaseda 1995).

Except the ENSO (2—7 a) component, according to the wavelet analysis, Nino3 index or the time series of global mean SST has a very broad spectrum ranging from 8 years to 100 years. There are three peaks centered near 10, 21, and 42 years, respectively (Lau and Weng 1999). Latif and Barnett (1996) pointed out that the decadal mode in the midlatitude oceans played a role in the tropical oceans. Latif et al. (1997) also marked out a decadal horseshoe pattern in association with the SSTA in the first half of the 1990s. Recently, there are several papers to address the tropical Pacific decadal, or multidecadal variability of SST and its relationship with the ENSO phenomenon (Trenberth and Hurrell 1994; Wang and Ropelewski 1995; Graham 1994; Lau and Weng 1999; Zhang et al. 1997; and Latif et al. 1997; Gu and Philander 1997; Gutzler 1996; Jacobs et al. 1994; Kleeman et al. 1999). It has been found that the ENSO exhibits interdecadal variation, not only the ENSO onset changes in the last four decades (Wang 1995) but also the frequency and amplitude (Trenberth and Hoar 1996; An and Jin 2000).

In this paper we aim to address the following questions: 1) what are the characteristics of the decadal oscillation in the tropical Pacific? 2) How does the decadal oscillation affect the ENSO signal? The paper is organized as follows: In Section II a brief introduction of data and methods is presented at first. An initial investigation of the decadal variation in the tropical Pacific is described and two different modes of decadal variability of the tropical oceans are identified. In Section III the decadal modes of the tropical atmosphere are investigated. Section IV is a discussion of the evolution of the decadal oscillation in the tropical Pacific in association with the atmospheric response. In Section V the possible relationship between tropical Pacific decadal oscillation and the ENSO signal is probed, and the mechanism by which the decadal variation acts on the ENSO is explored through both statistical and theoretical analyses. Conclusions and discussions are given in Section VI.

II. CHARACTERISTICS OF THE DECADAL VARIABILITY IN THE TROPICAL PACIFIC

In this section, the wavelet analysis was applied to the NCEP monthly mean SST data set that has the resolution of 1°×1° from January 1948 to June 1998, and NCEP reanalysis 850 hPa wind fields in the same period. As a filter, the wavelet approach can separate the ENSO signal of the 2—7 year period from the decadal mode of the 8—20 year period. Characteristics of the decadal variability of SST in the tropical Pacific and corresponding low-level wind features in the atmosphere are to be revealed.

1. *The Decadal Variability*

Figure 1a shows the Hovmoller diagram of the decadal component of the SSTA along the equator. An oscillation of the 10—15 year period can be identified, and maximum SST anomalies are located either near the dateline or in the eastern Pacific. Attention should be paid to the fact shown also in this figure that the two SSTA maximums are in phase or nearly in phase prior to the 1990s, i.e., the evolution of SSTA in the central Pacific is in accord with that in the eastern Pacific. However, during the 1990s the SSTA patterns in the two places shifted to be out of phase. From 1990 to 1995, positive SSTA of decadal scale dominates the equatorial central Pacific (ECP), while negative SSTA occupies the equatorial eastern Pacific (EEP). During this period, three relatively weak El Nino events

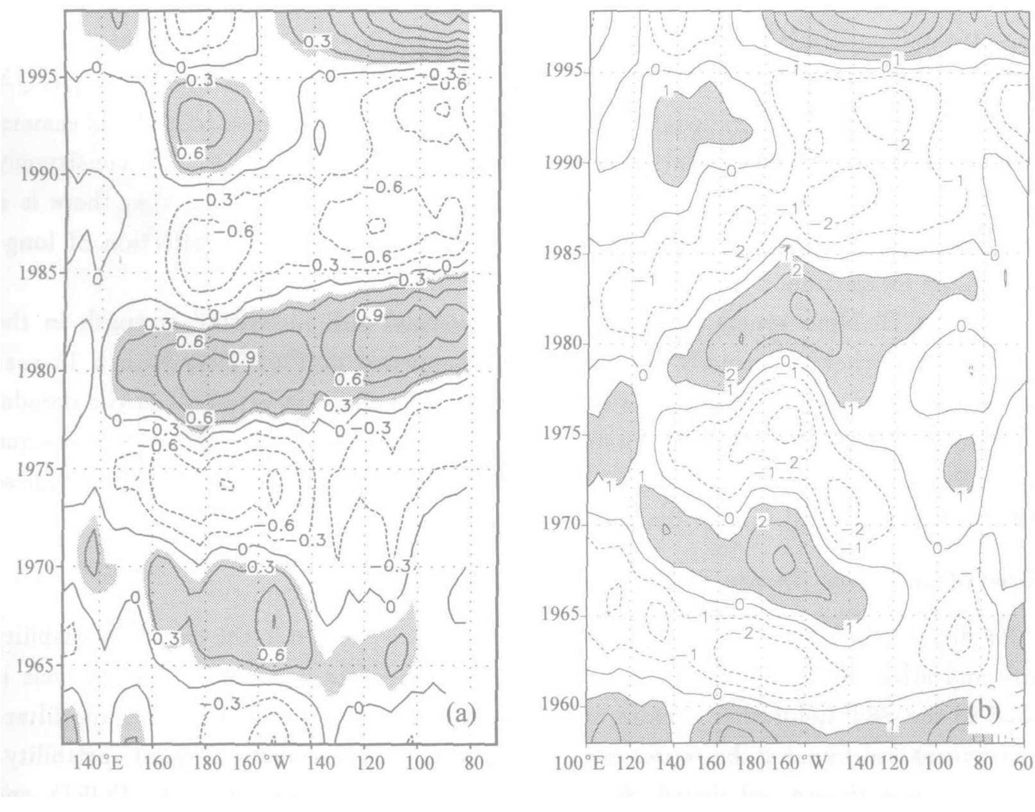

Fig. 1. Equator-time cross sections of SSTA decadal component (a) and 850 hPa zonal wind (b).

occurred, and major warming area was not located in EEP, but in ECP. This is fairly obvious for the 1993 and 1994/1995 El Nino events, and it could be associated with the decadal SSTA regime in the same period. Since 1995 the decadal oscillation occurred with opposite phase, that is, positive SSTA prevailed in EEP while negative SSTA occupied the ECP. This pattern may have contributed to the development of 1997/1998 El Nino, and made it even stronger than the 1982/1983 El Nino event. This could also be a factor that accelerates the subsequent attenuation of the 1997/1998 El Nino since the cold decadal SSTA experienced in the ECP. After reaching its peak in December 1997, positive SSTA in Nino1 and Nino2 areas still exists for a few months even though the negative SSTA has marched into Nino3 and Nino4 areas with the lowest value of -1°C or so.

A similar analysis was applied to the anomaly of the 850 hPa u component of the atmospheric wind field (referred to as UA from now on). As shown in Fig. 1b, the 10—15 year oscillation can also be identified in the evolution of UA. Comparing Fig. 1a and Fig. 1b, we can find that more intense decadal westerly anomalies took place over the region where warm decadal SSTA showed up. It was also found that prior to 1976 either the westerly or the easterly wind anomalies were initially generated in EEP, and then propagated westward. However, since 1976 the decadal UAs were generated first in western Pacific and propagated eastward instead. Since 1990 opposite decadal UA evolution patterns appear corresponding very well to those of SSTA. Specifically, from 1990 to 1995 the westerly UA dominated western Pacific while easterly UA occupied eastern Pacific. This forms a low-level convergent zone in central Pacific, which is very possibly associated with the three warm events in this period. After 1995 easterly UA occurred in the western Pacific while strong westerly UA controlled the central and eastern Pacific. This is in good agreement with the decadal warm SSTA in EEP. The consistency of changes in both oceans and atmosphere on the decadal scale indicates that there is a salient response of atmosphere to the oceanic forcing. This is also a reflection of long-range air-sea interaction.

Why the El Nino events occurred more frequently with increasing strength in the 1990s? Why another abnormally severe El Nino happened in 1997/1998 with a 15-year interval after the famous 1982/1983's event? Could it be that the variation of the decadal oscillation and the change of the sea temperature gradient between equatorial eastern and western Pacific have been conducive to the irregularity of ENSO cycle in the 1990s? These are the issues worthy of further inquisition.

2. *Two Modes of the Decadal Variability in the Tropical Pacific*

As discussed in Section II-1, there is a significant distinction in the decadal variability before and after 1990. This feature can also be clearly identified when EOF analysis is applied to the SST fields that contain only the decadal information after using the filter. Two patterns are found to be representative of the two modes of the decadal variability. Figure 2 shows the spatial distributions and time coefficients of the first (EOF1) and second (EOF2) eigenvalues of the decadal component of the tropical Pacific SSTA. EOF1 contributes 45% to the total variance, and its amplitude is much larger before 1990 than after 1990, thus EOF1 mainly represents the decadal mode of the tropical Pacific SSTA before 1990. A wide range of negative values extending northward and southward nearly to the coast of North and South America, and westward to the central Pacific is shown in

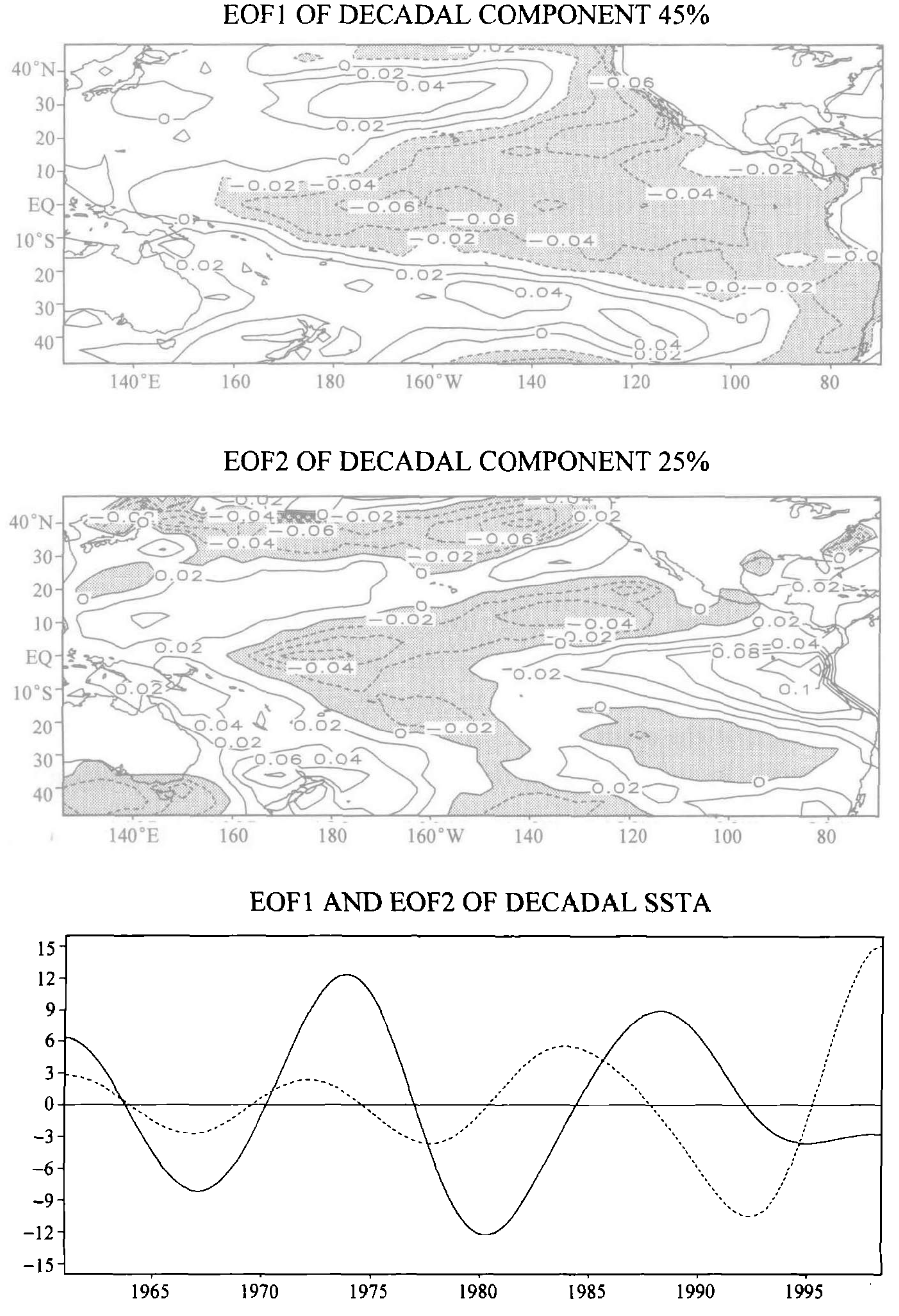

Fig. 2. The spatial distribution and time coefficient of the first EOF1 and second EOF2 of the SSTA decadal components for 1958—1998. Solid line represents EOF1, dashed line denotes EOF2.

EOF1. The positive values exist in the western Pacific and extratropical latitudes with two maximums located in the North and South Pacific respectively. This pattern is quite similar to the horseshoe pattern that was named and described by Latif et al. (1997) in seeking a characteristic pattern of the interdecadal variability. Here, we just follow their usage of the name. Since 1990, EOF2 has become a dominating mode and it bears increasing amplitude in contrast to that of EOF1. Starting from a constant variance contribution of 25%, the amplitude of EOF2 grows in the 1980s and tends to intensify faster in the 1990s. A distinctive feature in the horizontal distribution of EOF2 is that the decadal component of the SSTA variation has opposite signs between the eastern Pacific and the central Pacific. The positive centers appear along the coast of equatorial Central America in Nino1 and Nino2 regions. The negative centers are located near the dateline, stretching eastward, southward and northward by $\pm 20°$ in longitud or latitude, respectively. There are two negative anomaly centers occupying the North Pacific and South Pacific, replacing the positive centers in the horseshoe pattern of EOF1. Therefore, the EOF2 pattern may be called a horse saddle pattern and it is a dominating mode of the decadal variability in the 1990s.

Under this decadal climate background of the horse saddle pattern, it is understandable why all three El Nino events in the first five years of 1990s bore relatively weak intensity. The major reason could be that the reverse pattern of the decadal background offsets the warm SSTA in central Pacific and the cold SSTA in eastern Pacific during these events. The anomalous development of the 1997/1998 El Nino may be attributed to the fact that the distribution of the horse saddle decadal pattern, the warm SSTA in eastern Pacific and cold SSTA in the central Pacific, is superposition on the ENSO signal, and thus the event is intensified by the decadal variability. In this case, the decadal fluctuation is in phase with the ENSO cycle and provides a favorable setting for its significant development.

As stated above, the decadal SSTA variability has two horizontal modes, the horseshoe pattern that dominated before 1990, and the horse saddle pattern that dominated during the1990s. We then further examine the relationship between the two modes. From the time coefficient curve it is seen that the EOF1 of the decadal component is in quadrant with the EOF2. The two eigenvectors are almost normal, particularly after 1970, i.e., when EOF1 reaches a peak or a valley value, EOF2 approaches zero, whereas EOF2 has a peak or valley, EOF1 achieves zero. Therefore, the two modes can be regarded as being representative of different phases of the decadal oscillation. If the horseshoe pattern is defined as the 1st phase (corresponding to positive SSTA) and the 3rd phase (corresponding to negative SSTA) of the decadal oscillation, then the horse saddle pattern is actually a transition phase, namely, the 2nd or the 4th phase. In fact, the two patterns exist all the time, except that the 1st and the 3rd phases reside for a long time before 1990, while after 1990, the 2nd and the 4th phases retain longer. The horseshoe and the horse saddle patterns are in virtually a pair of principal distribution modes for the decadal oscillation. The decadal components of the SSTA in 1980 (1997) and 1975 (1992), respectively, are typical horseshoe (horse saddle) modes (figure not shown).

Noticeably, each mode has two phases with resembling layouts, but with opposite signs, which are referred to as the positive mode and negative mode.

III. DECADAL VARIABILITY OF THE TROPICAL ATMOSPHERE

Corresponding to the tropical SSTA, the decadal component of the 850 hPa wind anomaly obtained with EOF analysis also has two major modes matching the horseshoe and horse saddle patterns of the SSTA field, as demonstrated in Fig. 3. Arrows indicate wind anomaly vectors obtained via the vector EOF decomposition. Shadings represent westerly anomaly area. In the EOF1 wind field, westerly anomalies dominate almost the whole equatorial Pacific, extending considerably northward towards the eastern Pacific. The meridional wind anomaly is fairly small, so the wind flows more or less zonally from west to east with a maximum westerly anomaly dwelling in the equatorial central Pacific. There is a cyclonic circulation system situated in the North Pacific with its center approaching the North American coastal area. This mid-latitude low-frequency system is closely related to the tropical atmospheric circulation, and it can be traced from the decadal oscillation of the SSTA as well. Comparing Fig. 2c with Fig. 3c, we can see that EOF1 of the decadal wind component is in close concordance with the horseshoe SSTA pattern. As a result of the long-term air-sea interaction, decadal wind fields seem to be generated to counteract the decadal SSTA variability.

Figure 3b shows a complex distribution of the EOF2 in which the westerly anomaly is located in the western Pacific and the easterly anomaly is located in the eastern Pacific. The meridional wind anomaly is apparently larger than that of the EOF1. A low-level convergent zone is formed from 160°W to 120°W along about 5°N. In the north and south of the equatorial western Pacific, there appears a pair of cyclonic circulation systems. Therefore, the westerly wind anomaly controls the equatorial region between 10 degrees of latitude poleward, while the easterly wind anomaly occupies the region from 10° to 25° and the decadal components of the SSTA in 1997 and 1992, respectively, are typical horse saddle patterns degree of latitude poleward. The cyclonic circulation system in the North Pacific still exists in the EOF2 as that in the EOF1, but it covers a smaller area, and its center shifts southward by nearly 10°. The EOF2 of the decadal wind anomaly pattern coincides with the horse saddle pattern of the decadal SSTA variability. The easterly wind anomaly area fits the negative SSTA area, and the westerly wind anomaly fits the positive SSTA area. The interaction of the atmosphere and ocean leads to a relatively complex distribution of the decadal wind component as compared with the decadal SSTA component. Generally speaking, the atmospheric wind fields tend to suppress the heating anomaly of the oceans and adjust them back to the climatological mean state.

The correlation between the decadal SSTA and wind anomaly obtained by using the singular value decomposition (SVD) method shows that temporal evolution of the SVD1 coefficient of the decadal SSTA is in fairly good agreement with that of the decadal wind anomaly. The averaged correlation coefficient is 0. 97 between the two time series (figure not shown). The same is true for SVD2 (figure not shown). The SVD1 and SVD2 horizontal layouts of the decadal SSTA are almost identical to EOF1 horseshoe pattern and EOF2 horse saddle pattern (Fig. 4a vs. Fig. 2a, Fig. 4c vs. Fig. 2b, respectively). The same is true to the decadal wind component (Fig. 4b vs. Fig. 3a, Fig. 4d vs. Fig. 3b). It is shown in Fig. 4b that the zonal wind anomaly prevails along the equatorial Pacific with two cyclonic circulation systems residing in the North Pacific and South Pacific, which corresponds very well to the EOF1 mode of the decadal wind fields. This horseshoe

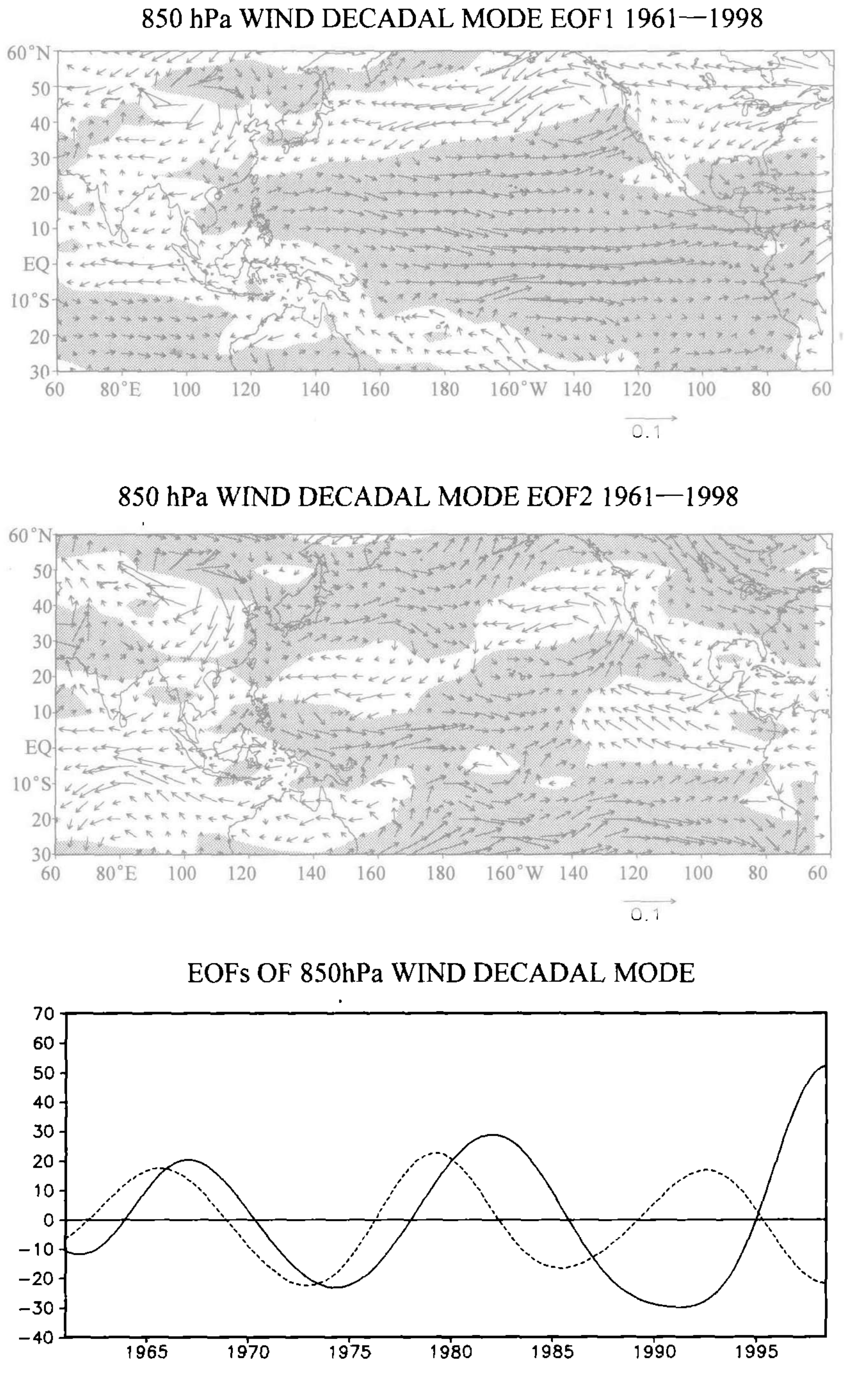

Fig. 3. As in Fig. 2, but for the 850 hPa wind.

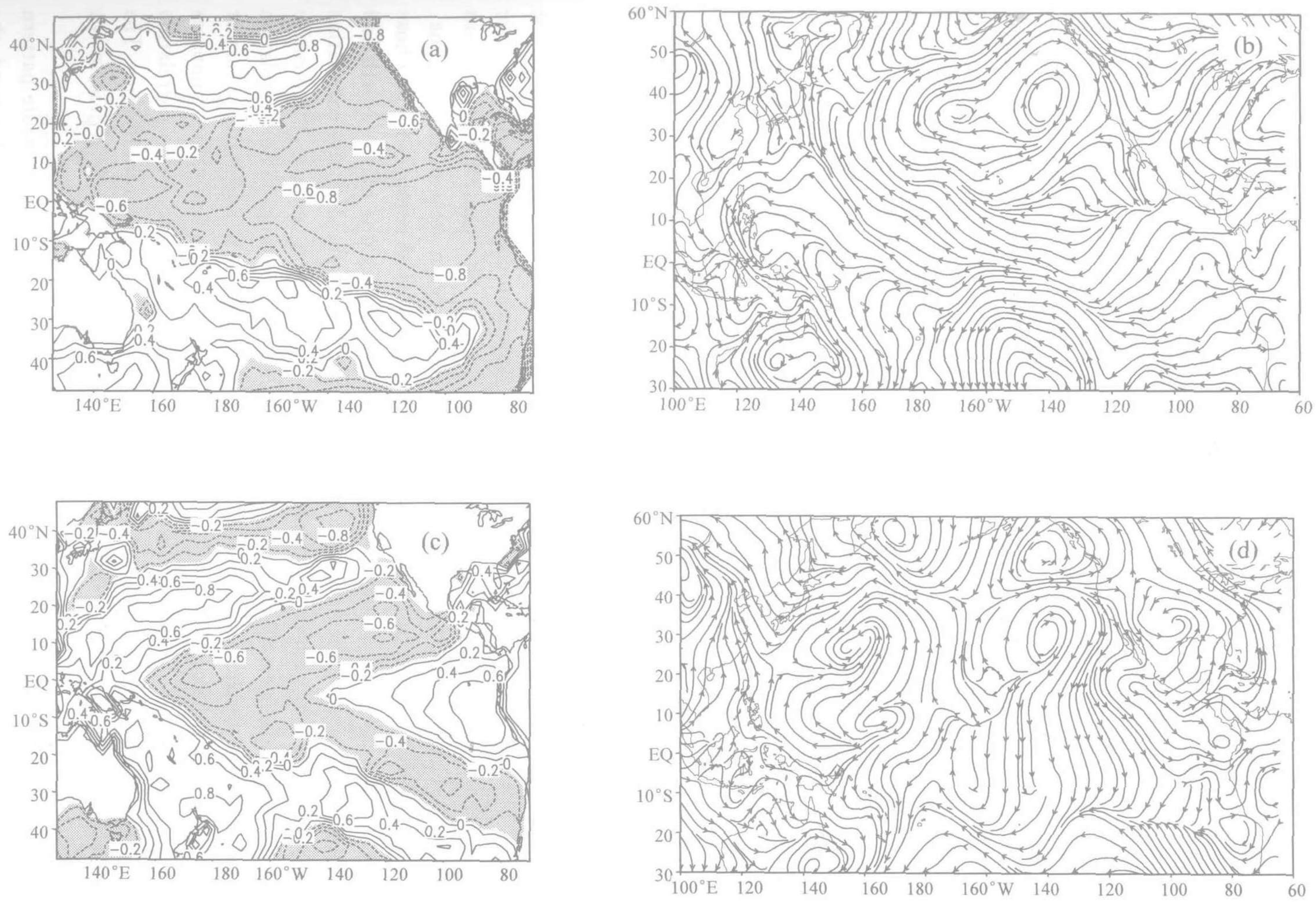

Fig.4. The first two correlation fields between the decadal SSTA and 850 hPa wind anomaly of SVD. (a) SVD1 of SSTA decadal component, (b) SVD1 of 850 hPa wind anomaly, (c) SVD2 of SSTA decadal component, (d) SVD2 of 850 hPa wind anomaly.

pattern accounts for 70% of the total variance, and it is a principal mode in decadal variability. Figure 4c illustrates that SVD2 of the decadal SSTA manifests virtually the horse saddle pattern of EOF2 SSTA decomposition, and correspondingly, the wind anomaly distribution is dominated by the meridional flow, which could be brought about by the SST gradient from the horse saddle pattern. Although the SVD2 mode contributes only 22% to the total variance, its amplitude rises considerably during the 1990s, in particular, after 1995. This may be one of the reasons why ENSO develops abnormally strong in the 1990s.

IV. THE EVOLUTION OF THE DECADAL VARIABILITY IN TROPICAL PACIFIC

As illustrated before, there are two modes of the decadal variability in the tropical ocean-atmospheric system: the horseshoe pattern and the horse saddle pattern. They represent different stages or phases of the decadal oscillation. We have calculated the correlation coefficients of the decadal component of the tropical Pacific SSTA with the decadal component of the Nino3 index. Figures 5a, 5b, 5c, and 5d show the point correlation relationship lagging six years, four years, two years and the concurrent point correlation, respectively. For the correlation lagging 6 years (Fig. 5a), it bears an analogous layout of reversed (or negative) horseshoe pattern as compared with the decadal SSTA. More specifically, the area of negative correlation occupies a large part of the equatorial Pacific, in particular the eastern Pacific. Largest negative correlation is shown in the central and western equatorial Pacific, with -0.6 as the maximum correlation coefficient, in contrast to -0.2 in the eastern Pacific. Extending southward and northward from the equatorial western Pacific two positive correlation bands sit in the North Pacific and South Pacific, with a maximum correlation of 0.8.

The correlation with four-year lag (Fig. 5b) displays the characteristics of the horse saddle pattern. In the eastern Pacific, along the South American coastal area the positive correlation is seen. The negative correlation still dominates the central and western equatorial Pacific, but the maximum shifts westward to the region west of the dateline. The positive correlation centers in the mid-latitudes are weakened as compared with those shown in Fig. 5a and spread eastward to approach the coastal regions of the North and South America. This is a manifestation of the horse saddle pattern. For the correlation lagging two years (Fig. 5c), except a couple of negative correlation centers, the positive correlation area extends westward and poleward to a great extent. The correlation coefficient is 0.6 in the eastern equatorial Pacific, and the negative correlation appears at the mid-latitudes. As to the concurrent correlation (Fig. 5d), the positive value dominates the whole equatorial zone and especially the tropical eastern Pacific. The correlation maximum comes to the value greater than 0.8 in the equatorial eastern Pacific. The negative correlation ranging form -0.6 to -0.8 occupies the mid-latitude region in the North and South Pacific.

The above analysis confirms that the horseshoe pattern and the horse saddle pattern are virtually varying phases of the decadal oscillation. We may as well regard the horseshoe pattern as the mature phase of the decadal oscillation, and the horse saddle pattern as the transition phase. On the other hand, the propagating feature of the decadal

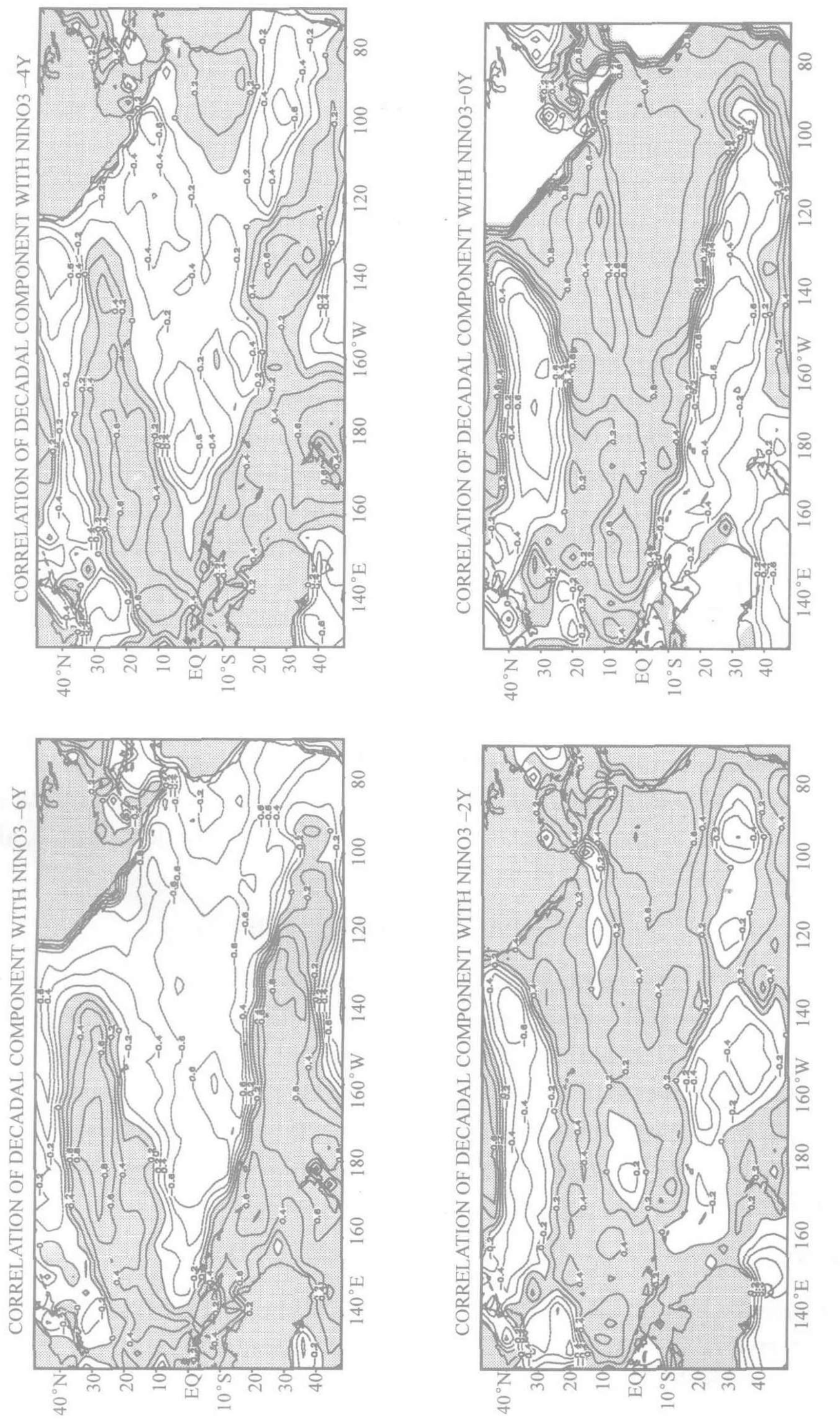

Fig. 5. The point correlation lagging 6 yrs. (a), 4 yrs. (b), 2 yrs. (c) and 0 yr. (d), respectively, of the SSTA decadal component with the decadal component of the Nino3 index.

variability is also worthy of attention. As shown in Fig. 5, the low-frequency component of the decadal oscillation propagates from east to west, expands poleward for a wide coverage of the tropical eastern Pacific, and usually gets intensified in the central equatorial Pacific. Furthermore, two varying centers of very low frequency move from west to east at the mid-latitudes, and exhibit somewhat a tilt toward the equator. Therefore, the generation, migration and dissipation of these three centers that act at a very low frequency constitute an evolution scenario of the tropical Pacific SSTA on the decadal time scale. The results support the idea proposed by White et al. (2000) that a delayed action oscillator mechanism shared by the decadal signal in the Pacific basin.

Being consistent with the above evolution scenario of the SSTA, the decadal component of the 850 hPa wind fields bears quite similar characteristics. The correlation of the decadal component of the 850 hPa wind vector with the decadal component of the Nino3 index (figure not shown) is demonstrated that the correlation with six-year lag displays a similar distribution to the concurrent correlation and the correlation leading six years. It is comparable to the horseshoe pattern shown in the decadal SSTA. A striking feature of this pattern is that zonal flow predominates the equatorial central and western Pacific with a consistent westerly flow found in the concurrent correlation and a consistent easterly flow found in the correlation leading or lagging six years. On the contrary, the correlation leading or lagging four years features the horse saddle pattern with meridional flow dominating. In addition, vortices and shears can be seen developing along the equator, and considerable exchange of airflow takes place between the Northern and the Southern Hemispheres. In conclusion, the zonal flow anomaly of the decadal component of the 850 hPa matches the horseshoe pattern of the decadal SSTA, whereas the meridional flow anomaly matches the horse saddle pattern. This consistency of SST and wind on the decadal scale is a result of the long-term ocean-atmosphere interaction, and is also an intrinsic feature of the coupled ocean-atmosphere system.

V. THE RELATIONSHIP BETWEEN DECADAL VARIABILITY AND ENSO

Latif et al. (1997) have pointed out that the anomalous ENSO cycles in the 1990s were controlled by the decadal modes. The decadal component of the observed SSTA in tropical Pacific during the first part of 1990s is characterized by the negative horse saddle pattern. The warm SSTA persists in the central Pacific for more than 4 years. However, during the late 1990s the positive horse saddle pattern dominated the tropical Pacific, and the warm SSTA in the eastern Pacific played a significant role in the anomalous El Nino development in 1997/1998.

1. *SVD Analysis*

To investigate the link of the decadal variability with the ENSO signal, the first two heterogeneous correlation modes of SVD between the decadal SSTA and the ENSO component are shown in Fig. 6. For SVD1, the time correlation coefficient reaches up to 0. 96, with the right fields resembling the horse saddle decadal pattern. The left field corresponds to spatial correlation of ENSO component that has a quite similar distribution with the same signs. It means that positive SST anomaly of ENSO warm phase is

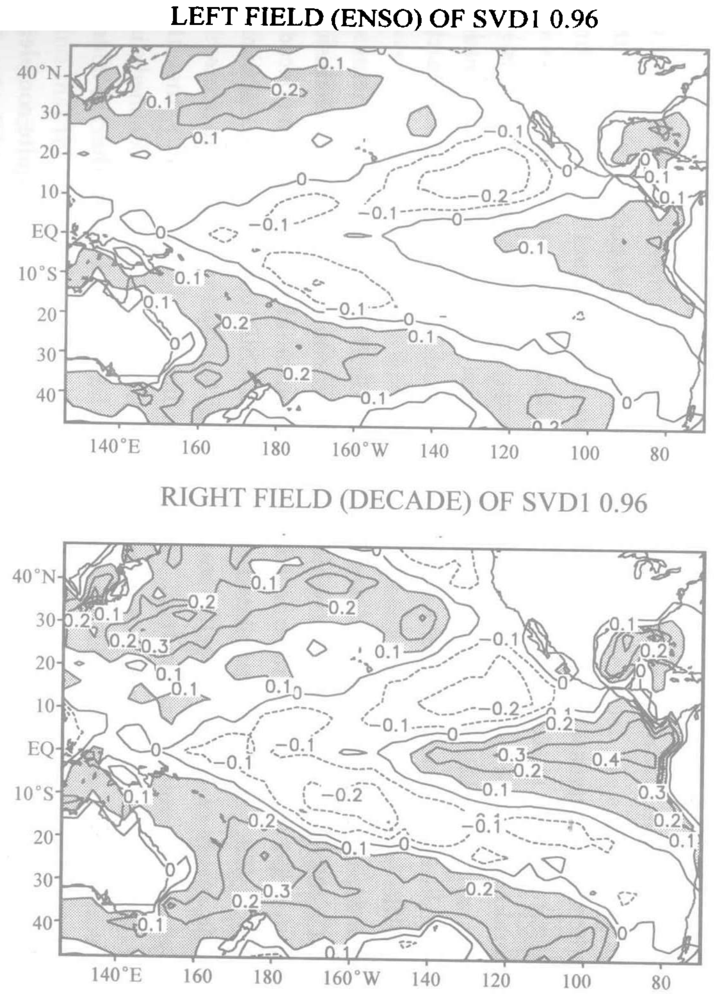

Fig.6a. Spatial correlation fields of SVD1 for ENSO componet with the decadal component.

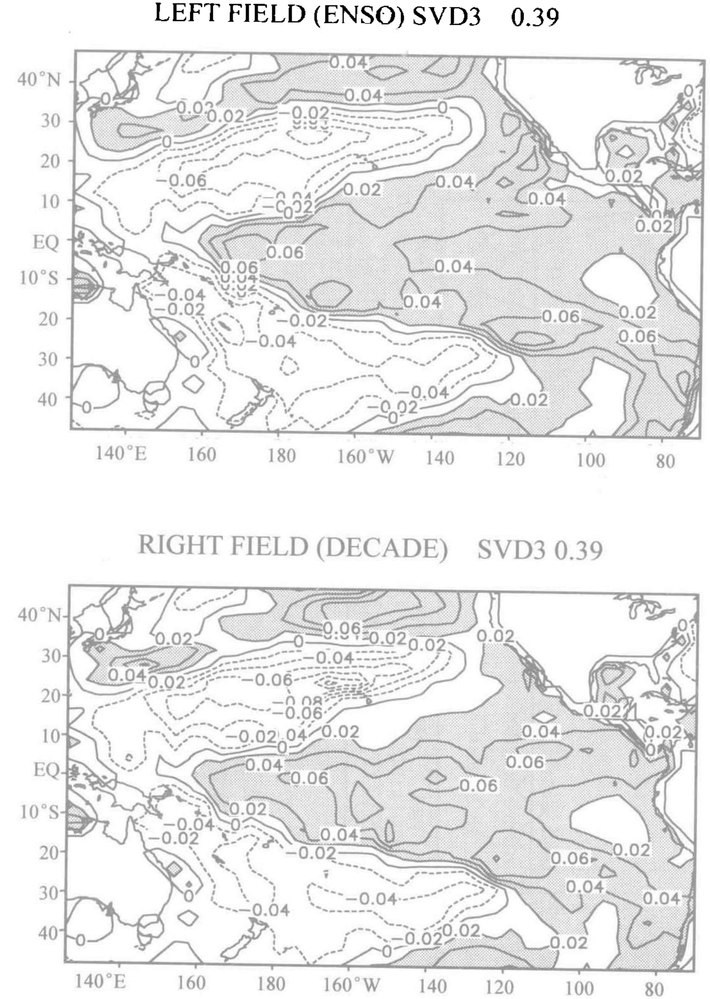

Fig.6b. As in Fig.6a, except for SVD3.

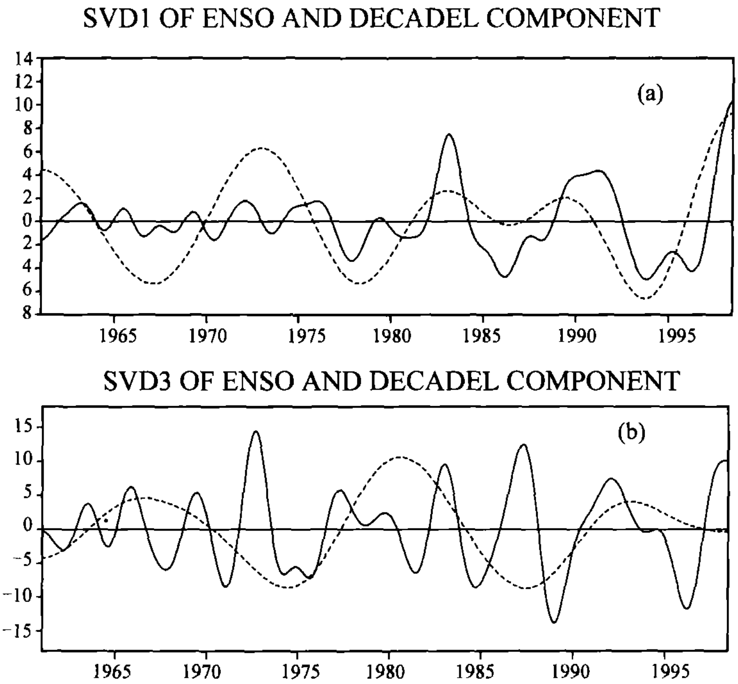

Fig. 6c. Time coefficient of SVD1 (a) and SVD3 (b). Solid lines represent ENSO time scale component and dashed lines denote decadal component.

simultaneously enhanced by the positive horse saddle decadal mode in the eastern Pacific and is reduced in the central Pacific (for example, the 1997/1998 El Nino event). The case is reverse for the negative SSTA of ENSO cold phase. On the other hand, the positive SSTA of the warm phase is decreased by the negative horse saddle decadal mode in the eastern Pacific and is increased in the central Pacific (such as, the 1991/1992 El Nino event). Opposite change is true for the cold phase of ENSO. If we look at the curves of SVD1 temporal coefficient in Fig. 6c (upper panel) and pay more attention to the 1990s, it can be found that the SVD1 of ENSO time scale field (solid line) varies with the decadal component (dashed line) in much the same phase, and both are more significant in the 1990s than in the 1980s.

The second pair of SVD modes shown in Fig. 6b indicates that two components of SSTA exhibit a low correlation of 0.39, which is somewhat coincident with the conclusion of Latif et al. (1997). The horseshoe decadal pattern can be identified from the decadal field of SVD3. The spatially correlated regions of ENSO component are similar. Comparing the curves of temporal coefficient SVD3 (Fig. 6c, bottom panel), it is easy to see that they evolve independently from each other. The solid line exhibits that the behavior of ENSO cycle well matches the observation of Nino3 and the dashed line demonstrates an oscillation on decadal time scale, with large amplitude in the 1980s and smaller amplitude in the 1990s.

The relationship between the ENSO signal and the decadal variation is quite complex, but we can make two points from the above analysis: first is that the horse saddle decadal mode may exert a greater influence on the ENSO component than the horseshoe mode.

Second is that the canonic ENSO events of 1990s are strongly linked with the more active horse saddle mode during this period.

2. Mechanism of How the Decadal Variability Affects the ENSO

Based on the diagnostic analysis of SSTA in above sections, the characteristics of decadal modes and their relationship with the ENSO signal have been disclosed. But the question of why the two decadal modes have different influences on the ENSO is still open. In this section, we will focus on the mechanism of the influence of the decadal variability on the ENSO by analysis of the observational subsurface temperature data (White 1995).

The two most significant EOF modes of subsurface temperature anomaly (STA) on 0 —400 m depth along the equator in the period of 1955—1998 (figure not shown) suggest that the pattern of EOF1 is associated with the ENSO phenomenon and accounts for about 38% of the total STA variance. There is a positive anomaly from the sea surface down to 150 m deep in the central and eastern equatorial Pacific with the maximum occurring at 50 m depth near the eastern thermocline. But a negative STA center at 150 m depth is found along the western equator. The STA associated with the ENSO mode evolves basically as a Kelvin wave propagating eastward, with a weak anomaly occurring first in the equatorial western Pacific and then moving eastward. The STA during the ENSO extremes is strongest in the equatorial eastern Pacific, with weaker anomaly of the opposite sign in the equatorial western Pacific. This means that the thermocline descends in the equatorial eastern Pacific and ascends in the equatorial western Pacific during El Nino phases. In contrast, the opposite movement of thermocline is observed during La Nina phases. The time series of EOF1 coefficient clearly show the observed extremes of the ENSO signal. Although the EOF1 mode does not provide any new information, we display it here to compare with other variability modes.

EOF2 is characterized by that a strong positive STA appears in the western and central equator with the central axis lying on the thermocline, and the maximum at the central Pacific. The EOF2's time coefficient oscillates in opposite to that of EOF1 almost everywhere, but with a few months lagging. We would like to emphasize that the EOF2 mode becomes stronger after the 1980s. This pattern causes the thermocline rise in the western and central equator and decline in the eastern equator when the ENSO warm phase occurs. Therefore, both EOF1 and EOF2 modes show a link with the ENSO signal, especially the latter, which has the extremes as the ENSO after the 1980s.

Similar analysis method has been applied to the time series of decadal component of the STA field (Fig. 7). The EOF1 spatial distribution demonstrates two positive centers in the central and eastern equator respectively and a negative center in the western Pacific. It accounts for about 47% of the total variance. This structure suggests that the thermocline in the central and eastern Pacific migrates up or down simultaneously with the horseshoe mode of SSTA very well. If this decadal EOF1 pattern is added to the ENSO cycle, we can find that the thermocline in eastern and central equator only moves in parallel a little up or down, so that the extremes of ENSO cycle can hardly be affected.

The STA decadal component of EOF2 spatial distribution appears in opposite sign in the central and eastern Pacific along the thermocline with a contribution of 29% to the

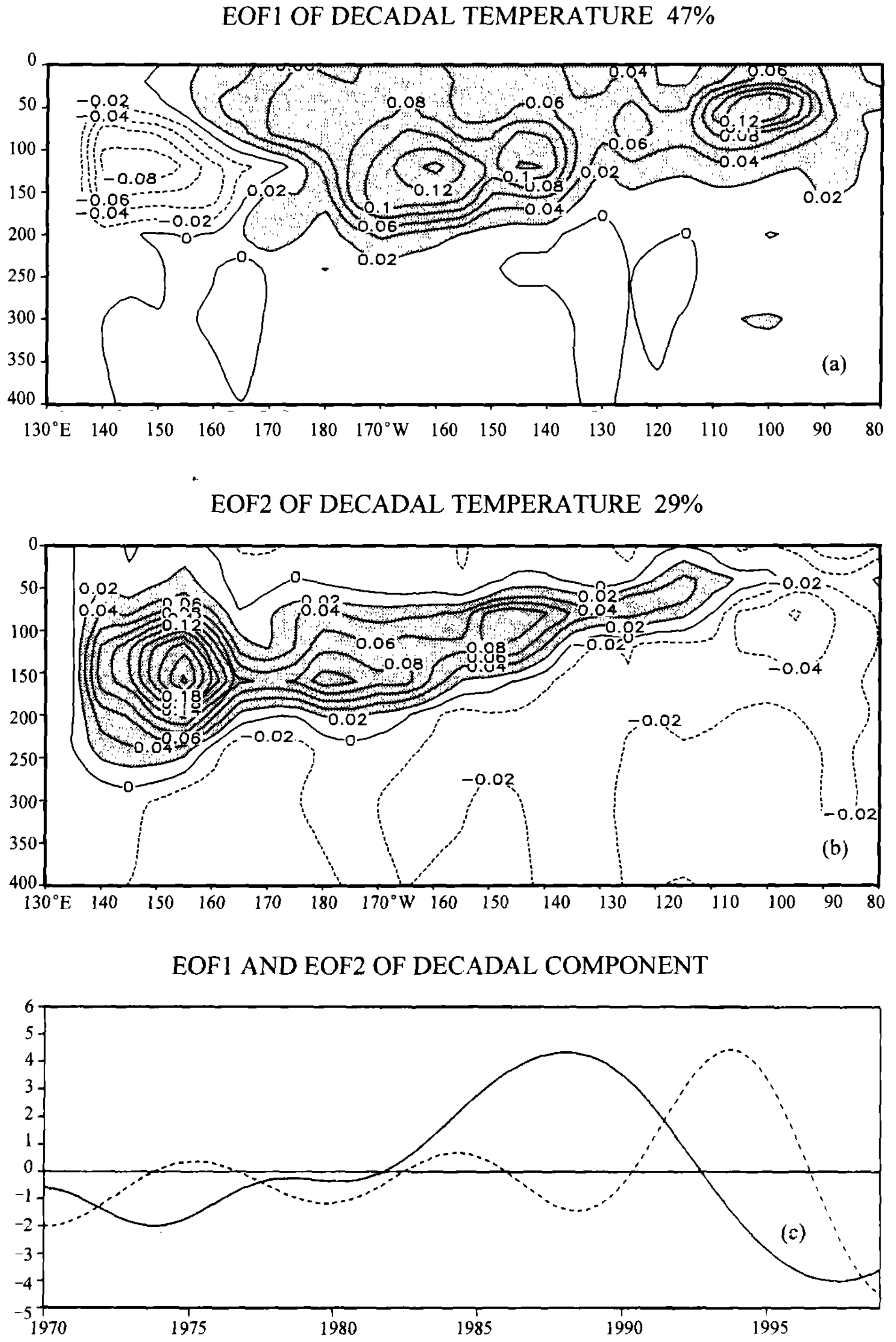

Fig. 7. The first two EOF decadal modes of 0—400 m depth XBT's subsurface temperature anomaly along the equator in period 1995—1998. (a) EOF1 mode, (b) EOF2 mode and (c) curves of time coefficients (siolid line represents EOF1, dashed line denotes EOF2).

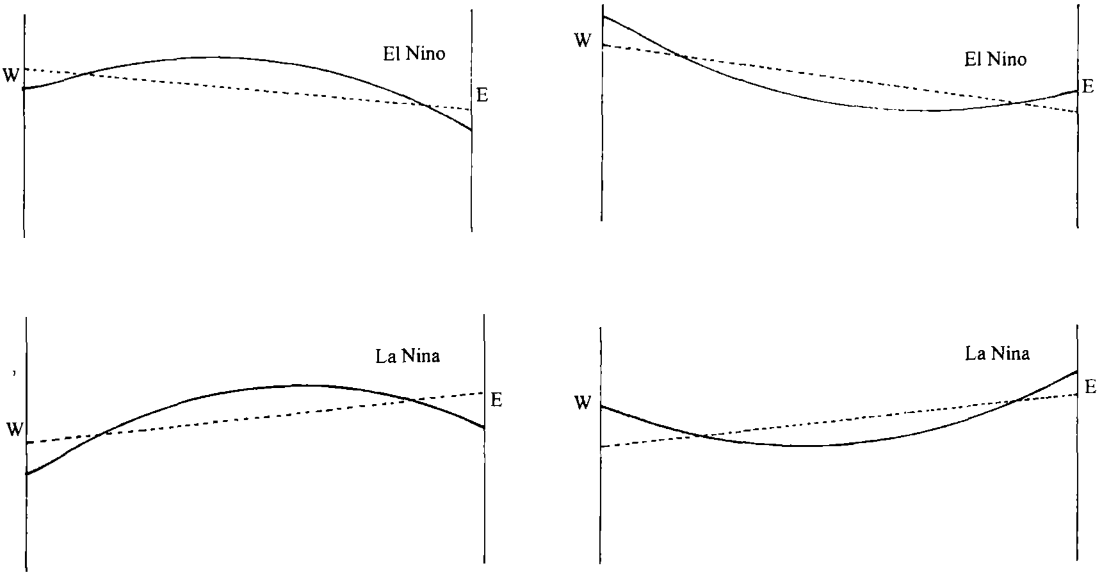

Fig. 8. Schemes of the horse saddle decadal mode influence on ENSO cycle.

total variance. This structure suggests that the thermocline in the central and eastern Pacific migrates in contradiction to the horse saddle SSTA decadal mode. The depth gradient of the thermocline is changed because it bends down in the central and rises up in the eastern equator. If this decadal mode as the climate background is superposed to ENSO cycle mode, the intensity of the ENSO cycle is to be altered. A schematic explanation is shown in Fig. 8. It enhances the amplitude of El Nino events or reduces that of La Nina when the thermocline moves up in the central and down in the eastern equator, which corresponds to the positive horse saddle decadal mode of SSTA. The reversal is true for the negative mode. For example, three El Nino episodes occurring in the early 1990s are actually weakened by the negative horse saddle decadal mode and the 1997/1998 El Nino episode seems strengthened by the positive horse saddle mode.

At last, in order to further document this point, the difference between the averaged STA for 1991—1995 and that for 1996—1998 is conducted (figure not shown). It is true for the positive STA in the central Pacific and the negative STA in the eastern Pacific along the thermocline, which curves down in the early 1990s firstly and then down in the late 1990s in the eastern Pacific. The case is reverse in the central Pacific. Therefore, the decadal variation affects the ENSO signal by reducing the El Nino amplitude in the early 1990s and enhancing it in the later 1990s.

VI. SUMMARY AND DISCUSSION

We have explored characteristics of the SST in the tropical Pacific and the low-level wind in the tropical atmosphere on the decadal time scale by using SST and 850 hPa wind data from 1948 to 1998. The major conclusions are as follows:

(1) There are two modes or two patterns, namely, the horseshoe pattern, and the horse saddle pattern, characterized with the decadal components of the tropical Pacific

SSTA and atmospheric low-level wind anomalies. The horseshoe pattern dominates prior to 1990, but after 1990, the horse saddle pattern dominates. The former corresponds to the zonal flow anomaly while the latter corresponds to the meridional flow anomaly.

(2) For the horseshoe pattern the decadal variability in the central Pacific is in phase with that in the eastern Pacific, but for the horse saddle pattern they are out of phase to each other.

(3) The two modes represent different phases of the decadal oscillation in the tropical Pacific, and this low-frequency variability is a result of the long-term air-sea interaction between the tropic Pacific and the ambient atmosphere.

(4) Evidence from diagnostics of observation data shows that influences of the two decadal modes on the ENSO signal are different. The horse saddle mode has stronger impact on the ENSO than the horseshoe in the 1990s. The anomalous development of ENSO in the 1990s is attributed principally to the horse saddle decadal mode.

(5) A possible mechanism for the influence of the decadal oscillation on ENSO signal is suggested by analysis of the STA along the equator, which demonstrates the decadal change of the thermocline in the tropical Pacific. When the thermocline moves up or down simultaneously in the central and the eastern tropical Pacific the decadal variability has little effect on ENSO. When it gets bended oppositely in the central and the eastern tropical Pacific, which is corresponding to the horse saddle mode, the decadal variability has a strong influence on ENSO.

Recently several papers have addressed the decadal or interdecadal variability of SSTA and its relationship with the ENSO (Lau and Weng 1999, Zhang et al. 1997 and Latif et al. 1997). The ENSO signal has already been clearly defined as a 2—7 year component of the tropical ocean-atmosphere oscillation system. However, up till now there is no strict definition about the time spans of the decadal or interdecadal variability. According to the wavelet analysis of Nino3 index or the time series of global mean temperature or global mean SST, a very broad wavelet spectrum ranging from 8 years to 100 years exists. There are three peaks centered near 10, 21, and 42 years, respectively (Lau and Weng 1999). In our study, we focused on the 8—20 year period for investigating the relationship between the decadal variability and the ENSO signal.

This decadal oscillation seems to be independent of the ENSO signal and may have a greater impact on it rather than that suggested in Latif's work (Latif 1997; Fig. 13). We can argue that the decadal oscillation Latif defined might be blurred by longer timescale variabilities, for example, the interdecadal signal or the global warming.

Although the term "horseshoe pattern" is used in this paper after Latif (1997), the difference of the spatial distributions can be found between his study and our work. The main point is that the strongest decadal variability is found along the equator and in the central Pacific in our study, which is similar to Zhang's (1997) results based on the analysis of 1900—1993 ENSO-like interdecadal variability. The horse saddle decadal mode proposed here has certain influence on ENSO, which helps us understand 1990s canonical El Nino events, but more work would be required to establish higher confidence identifying the horse saddle mode from decadal variability.

The impact of the two decadal modes on ENSO signal is discussed in this paper, and a simple relationship between the decadal mode and ENSO is identified by both observation data and a hybrid coupled model (not shown here). We conclude that the decadal mode is one of the sources of ENSO irregularity. but how it exactly interacts with ENSO on two different time scales remains to be understood.

We are grateful to Ms. YANG Qu for typing this paper and Mr. Jim MAKA kindly refining the English. We would like to thank Dr. WANG Dongxiao for assistance with the SAT data and Prof. NI Yunqi for insightful discussion. We would also like to thank JEDAC and FSU for data supply.

REFERENCES

An, S. and Jin, F. (2000), An eigen analysis of the interdecadal changes in the structure and frequency of ENSO mode, *Geophys. Res. Lett.*, **27**: 2573—2576.

Balmaseda, M. A., Anderson, D. L. T. and Davey, M. K. (1994), ENSO prediction using a dynamical ocean model coupled to statistical atmospheres, *Tellus*, **46A**: 497—511.

Balmaseda, M. A., Davey, M. K. and Anderson, D. L. T. (1995), Decadal and seasonal dependence of ENSO prediction skill, *J. Climate*, **8**: 2705—2715.

Barnett, T. P., Graham, N. E., Cane, M. A. Zebiak, S. E., Dolan, S. C., O'Brien, J. J. and Legler, D. M. (1988), On the prediction of the El Nino of 1986—1987, *Science*, **241**: 192—196.

Barnston, A. G., van den Dool, H. M., Zebiak, S. E., Barnett, T. P., Ji, M., Rodenhuis, D. R., Cane, M. A., Leetmaa, A., Graham, N. E., Ropelewski, C. R., Kousky, V. E., O'Lenic, E. A. and Livezey, R. E. (1994), Long-lead seasonal forecasts—Where do we stand? *Bull. Amer. Meteor. Soc.*, **75**: 2097—2114.

Cane, M. A., Zebiak, S. E. and Dolan, S. C. (1986), Experimental forecasts of El Nino, *Nature*, **321**: 827—832.

Graham, N. E. (1994), Decadal-scale climate variability in the 1970s and 1980s: Observations and model results, *Climate Dyn.*, **10**: 135—162.

Gu, D. and Philander, S. G. H. (1997), Interdecadal climate fluctuations that depend on exchanges between the tropics and extratropics, *Science*, **275**: 805—807.

Gutzler, D. S. (1996), Low-frequency ocean-atmosphere variability across the tropical western Pacific, *J. Atmos. Sci.*, **53**: 2773—2785.

Jacobs, G. A., Hurlburt, H. E., Kindle, J. C., Metzger, E. J., Mitchell, J. L., Teague, W. J. and Wallcraft, A. J. (1994), Decadal-scale trans-Pacific propagation and warming effects of an El Nino anomaly, *Nature*, **370**: 360—363.

Ji, M., Kumar A. and Leetmaa, A. (1994), An experimental coupled forecast system at the National Meteorological Center: Some early results, *Tellus*, **46**A: 398—418.

Ji, M., Leetmaa, A. and Kousky, V. E. (1996). Coupled model predictions of ENSO during the 1980s and the 1990s at the National Centers for Environmental Prediction, *J. Climate*, **9**: 3105—3120.

Kleeman, R., McCreary, J. P. and Klinger, B. A. (1999), A mechanism for generating ENSO decadal variability, *Geophys. Res. Lett.*, **26**: 1743—1746.

Latif, M. and Barnett, T. P. (1996), Decadal climate variability over the North Pacific and North America: Dynamics and predictability, *J. Climate*, **9**: 2407—2423.

Latif, M., Kleeman, R. and Eckert, C. (1997), Greenhouse warming interdecadal variability or El Nino? An attempt to understand the anomalous 1990s, *J. Climate*, **10**: 2221—2239.

Lau, K. M. and Weng, H. (1999), Interannual, decadal-interdecadal, and global warming signals in sea surface temperature during 1955—1997, *J. Climate*, **12**: 1257—1267.

Mason, S. J., Goddard, L., Graham, N. E., Yulaeva, E., Sun, L. and Arkin, P. A. (1999), The IRI seasonal climate prediction system and the 1997/1998 El Nino event, *Bull. Amer. Meteor. Soc.*,

80: 1853—1873.

Trenberth, K. E. and Hurrell, J. W. (1994), Decadal atmosphere-ocean variations in the Pacific, *Climate Dyn.*, **9**: 303—319.

Trenberth, K. E. and Hoar, T. J. (1996), The 1990—1995 El Nino-Southern Oscillation event: Longest on record, *Geophys. Res. Lett.*, **23**: 57—60.

Wang, B. (1995), Interdecadal changes in El Nino onset in the last four decades, *J. Climate*, **8**: 267—285.

Wang, X. L. and Ropelewski, C. F. (1995), An assessment of ENSO-scale secular variability, *J. Climate*, **8**: 1584—1599.

White, W. B., Tourre, Y. M., Rajagopalan, B., Kushnir, Y. and Barlow, M. (2000), A delayed action oscillator mechanism shared by biennial, interannual, and decadal signals in the Pacific basin, Submitted to *J. Climate*.

Zhang, Y., Wallace, J. M. and Battisti, D. S. (1997), ENSO-like interdecadal variability: 1900—1993, *J. Climate*, **10**: 1004—1020.